  Bull. Chem. Soc. Jpn., 59, 3367—3373 (1986)

Phase Transition of Unsymmetric Bis(quaternary alkyl bromide) Salts of 1,4-Diazabicyclo[2.2.2]octane, C_{10}-DABCO-C_n-Br_2 ($11 \leqq n \leqq 22$)

Jun SHIMIZU, Kengo IMAMURA, Takashi NOGAMI,* and Hiroshi MIKAWA†
Department of Applied Chemistry, Faculty of Engineering, Osaka University, Yamada-oka, Suita, Osaka 565
(Received April 23, 1986)

Phase transitions of unsymmetric bis(quaternary alkyl bromide) salts of 1,4-diazabicyclo[2.2.2]octane (DABCO)(C_{10}-DABCO-C_n-Br_2, $11 \leqq n \leqq 22$) were studied on the basis of measurements of differential scanning calorimetries, infrared absorption spectroscopy, and bromide-anion conductivities. The DSC measurements showed two transition temperatures (T_{c1} and T_{c2}, $T_{c1} > T_{c2}$); this exhibits the existence of the metastable phase for the DABCO salts (C_{10}-DABCO-C_n-Br_2, $12 \leqq n \leqq 22$). The metastable phase was converted to the stable phase within several days except for C_{10}-DABCO-C_n-Br_2 (n=12, 22). The temperature dependence of the infrared absorption spectra revealed that the band progressions due to two different alkyl chains disappeared at T_{c1} and appeared again at T_{c2}. This shows that the *trans*-zigzag conformation of the alkyl chains in the low temperature phase is destroyed by the conformational change above T_{c1} and then recovered again below T_{c2}. Abrupt increases in the bromide-anion conductivities by 100—1380 times were observed at around T_{c2} for the samples annealed beforehand above T_{c1}. However, the virgin samples showed much broader increases in the conductivities below T_{c1}; no conductivity jump was observed. The conductivity increase was caused by the conformational change in the alkyl groups. The concomitant formations of the voids facilitate the bromide-anion transport.

As an extension of the studies of the halide-anion conductivities of crown ether–metal halide complexes,[1] cryptand 222-metal halide complexes,[2] quaternary tetraalkylammonium halides,[3] and quaternary tetraalkylphosphonium halides,[4] we have studied the halide-anion conductivities of the symmetric bis(quaternary alkyl halide) salts of 1,4-diazabicyclo[2.2.2]octane (DABCO).[5] A first order solid-solid phase transition was observed for the DABCO salts, with concomitant increases in the halide-anion conductivities by two to three orders of magnitude. The phase transition was also studied by means of DSC, IR absorption spectroscopy, and powdered X-ray diffraction. The temperature dependence of the IR absorption spectra of the DABCO salts exhibited the abrupt disappearance of the band progressions above the transition temperatures.[6] Thus, the phase transition was found to be caused by the conformational change in the alkyl groups. Powdered X-ray diffraction revealed a reversible change in the crystal structure at the transition temperature.[5] Unlike the case of the symmetric salts, the existence of the metastable phase was clarified for the unsymmetric bis(quaternary alkyl bromide) salts of DABCO by means of DSC and a study of the IR absorption spectra.[7] The unsymmetric DABCO bromide salts studied previously possess two alkyl groups; the difference in their carbon numbers was fixed at two.[7] Since the unsymmetric salts exhibited different phenomena from the symmetric salts for the phase transition, it seemed interesting to see how the phase transition would be modified for the unsymmetric salts by changing the difference in the carbon numbers of two alkyl groups attached to DABCO nitrogens. The unsymmetric DABCO bromide salts in this study possess two alkyl groups; one is fixed to the decyl group, while the other is changed systematically from n-$C_{11}H_{23}$ to n-$C_{22}H_{45}$. The materials studied are shown in Fig. 1. The names of the materials are abbreviated by the numbers of alkyl carbons. For example, *N*-decyl-*N'*-tetradecyl-1,4-diazoniabicyclo[2.2.2]octane dibromide is abbreviated as C_{10}-DABCO-C_{14}-Br_2. Thus, the materials in Fig. 1 can be described generally as C_{10}-DABCO-C_n-Br_2 ($11 \leqq n \leqq 22$).

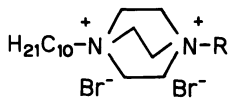

R = $C_{11}H_{23}$. $C_{12}H_{25}$. $C_{13}H_{27}$
$C_{14}H_{29}$. $C_{15}H_{31}$. $C_{16}H_{33}$
$C_{17}H_{35}$. $C_{18}H_{37}$. $C_{22}H_{45}$

Fig. 1. Unsymmetric bis(quaternary alkyl bromide) salts of DABCO.

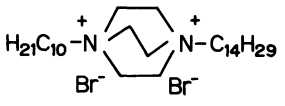

C_{10}-DABCO-C_{14}-Br_2

Experimental

Materials. All of the materials and the solvents were purified before the synthesis of the quaternary DABCO salts, as has been described previously.[6,7]

† Present address: Department of Environment and Safety Engineering, Faculty of Engineering, Fukui Institute of Technology, Gakuen-cho, Fukui 910.

Syntheses of Unsymmetric Bis(quaternary Alkyl Bromide) Salts of DABCO. The syntheses of mono(quaternary alkyl bromide) salts of DABCO were described in a previous paper.[7] The unsymmetric bis(quaternary alkyl bromide) salt of DABCO was synthesized by the reaction of the mono(quaternary salt) with alkyl bromide. The synthesis of unsymmetric salts will be described for C_{10}-DABCO-C_{14}-Br_2 as a typical example. The methanol (20 ml) solution of *N*-decyl-1-aza-4-azoniabicyclo[2.2.2]octane bromide (2 g, 6 mmol) and tetradecyl bromide (1.66 g, 6 mmol) was refluxed for 48 h. After it had then been cooled to room temperature, it was poured into diethyl ether (500 ml) to obtain a white precipitate. The crude product was recrystallized three times from the mixed solvent of ethyl acetate and ethanol (5:1). Essentially the same reaction conditions were adopted for the other materials. The solvents of recrystallization are acetonitrile for C_{10}-DABCO-C_n-Br_2 (n=11, 12, 13, 15, 16, 17, 18) and a mixed solvent of ethyl acetate and ethyl alcohol (5:1) for C_{10}-DABCO-C_n-Br_2 (n=14, 22) respectively.

Measurements. The measurements of the bromide-anion conductivities, DSC, and IR spectra were made by the methods described before.[5,6]

Results and Discussion

DSC Measurements. The DSC measurements were made while changing the temperature by 5 °C min^{-1}. Most of the virgin samples (C_{10}-DABCO-C_n-Br_2, $n \geqq 13$) showed single and reproducible endothermic signals (the values are designated as $\Delta H_{en,1}$) at the transition temperatures (designated as T_{c1}) when they were heated from room temperature. When they were cooled after they had once been heated above T_{c1}, much smaller exothermic signals ($\Delta H_{exo,1}$) were observed at much lower temperatures (T_{c2}) than T_{c1}; i.e., $\Delta H_{en,1} > \Delta H_{exo,1}$, and $T_{c1} > T_{c2}$. The succeeding heating-cooling cycles showed reproducible endothermic ($\Delta H_{en,2}$) and exothermic ($\Delta H_{exo,1}$) signals at around T_{c2}. The absolute values of $\Delta H_{en,2}$ were close to those of $\Delta H_{exo,1}$. Figure 2 shows the observed result of C_{10}-DABCO-C_{18}-Br_2 as a typical example of the above observations (T_{c1}=86 °C, T_{c2}=34 °C). However, when most of the samples ($13 \leqq n \leqq 18$) were kept at room temperature after they had once been heated above T_{c1}, the transition temperatures (T_{c2}) tended to increase slowly. After several days, the sample was converted to the original phase; it showed the endothermic signal ($\Delta H_{en,1}$) at T_{c1}. These facts can be explained by the free energy (F)-temperature (T) relation shown in Fig. 3. When the sample was heated from room temperature across the transition temperature, and then cooled, it followed the F-T curve by the sequence of 1→2→3→4→5 shown in Fig. 3. A detailed explanation of this F-T relation was given in the previous paper.[7] C_L, C_M, and C_H in Fig. 3 are the low temperature phase, the metastable phase, and the high-temperature phase respectively. The most important characteristic of the present materials is the existence of the metastable phase. The metastable phase was found to be converted to the stable phase (C_L) by keeping the sample at room temperature for several days. The gradual increase in the transition temperature can be explained as follows. When the C_M phase was left at room temperature, it was converted to another metastable phase ($C_{M'}$)[8] (Fig. 3). When a DSC measurement is made for the resultant $C_{M'}$ phase, its transition temperature ($T_{c2'}$) should be found between T_{c2} and T_{c1}; $T_{c2} < T_{c2'} < T_{c1}$. As the metastable phase approaches the C_L phase, the transition temperature increases until it is converted to the C_L phase where the phase transition takes place at T_{c1}. Thus, the greatest difference in the present systems (C_{10}-DABCO-C_n-Br_2, $13 \leqq n \leqq 18$) from the previous systems (C_n-DABCO-C_{n+2}-Br_2) is that the metastable phase can be converted to the stable phase in the former systems, whereas the conversion rate is too slow to be followed in the latter systems.[7] The larger the difference in the carbon numbers of the two alkyl groups, the faster was the conversion rate from

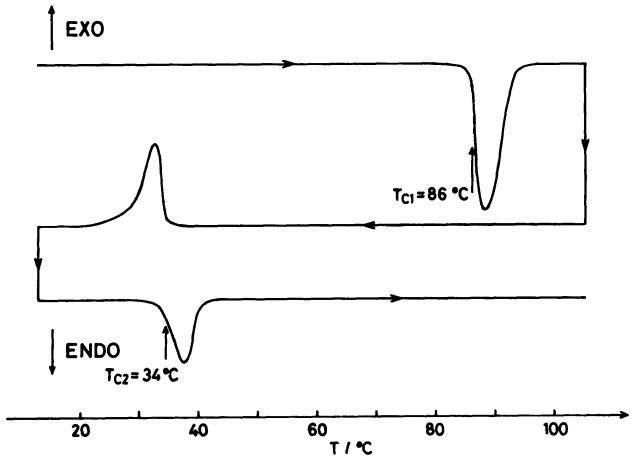

Fig. 2. DSC thermogram of C_{10}-DABCO-C_{18}-Br_2.

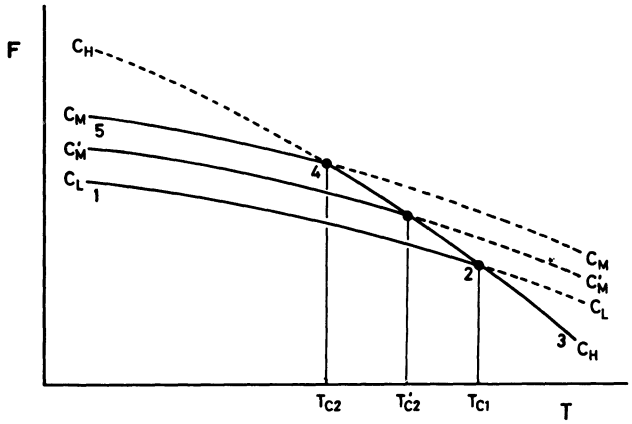

Fig. 3. Free energy (F)-temperature (T) relation of the unsymmetric bis(quaternary alkyl bromide) salts of DABCO. C_L, C_M, and C_H denote low temperature phase, metastable phase, and high temperature phase. respectively. C_M' denotes another metastable phase.

C_M to C_L.[9] For example, the conversion rates of C_{10}-DABCO-C_{14}-Br_2 and C_{10}-DABCO-C_{18}-Br_2 were one week and 1 d respectively. However, the C_M phases of C_{10}-DABCO-C_n-Br_2 (n=12, 22) did not go back to the C_L phases. C_M was not observed for C_{10}-DABCO-C_{11}-Br_2, which is similar to the cases of the symmetric bis(quaternary alkyl halide) salts of DABCO.[6]

Part of Table 1 shows some materials, T_{c1}, $\Delta H_{en,1}$, $\Delta S_1(=\Delta H_{en,1}/T_{c1})$, T_{c2}, $\Delta H_{en,2}$, and $\Delta S_2(=\Delta H_{en,2}/T_{c2})$. Here ΔS_1 and ΔS_2 denote the transition entropies at T_{c1} and T_{c2} respectively. The transition temperatures were obtained by the onsets of the endothermic peaks. The characteristic points of the salts are discussed below. Figure 4 plots T_{c1} and T_{c2} against the carbon

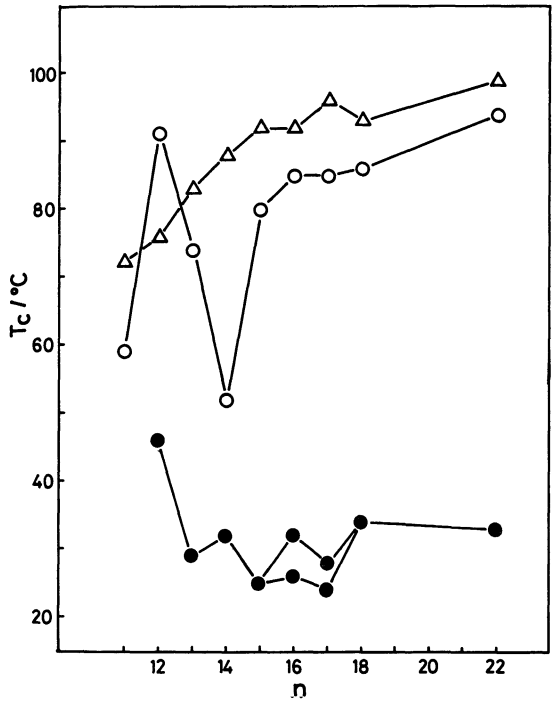

Fig. 4. The plots of the transition temperatures against the carbon numbers of alkyl groups.
○: T_{c1} for C_{10}-DABCO-C_n-Br_2, △: T_c for C_n-DABCO-C_n-Br_2, ●: T_{c2} for C_{10}-DABCO-C_n-Br_2.

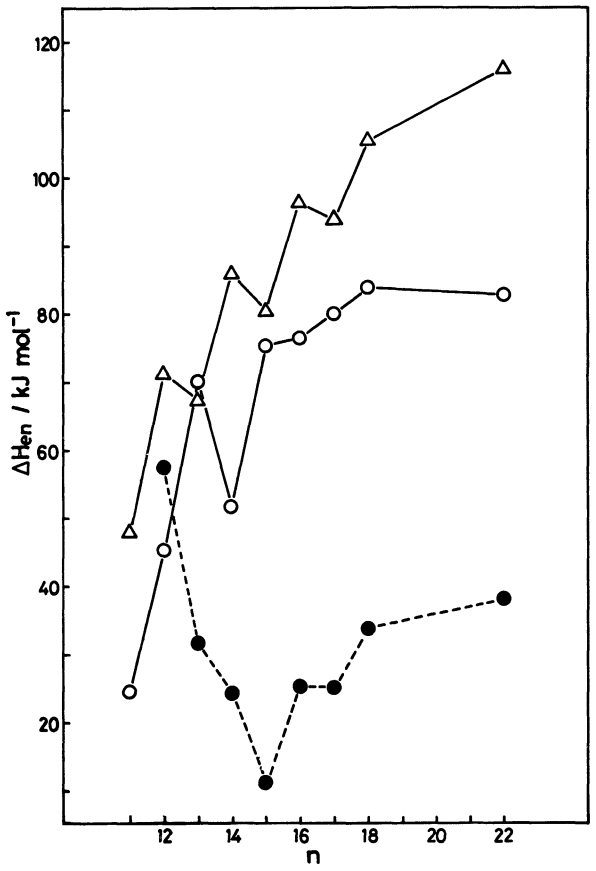

Fig. 5. The plots of the transition enthalpies against the carbon numbers of alkyl groups.
○: $\Delta H_{en,1}$ for C_{10}-DABCO-C_n-Br_2, △: ΔH for C_n-DABCO-C_n-Br_2, ●: $\Delta H_{en,2}$ for C_{10}-DABCO-C_n-Br_2.

Table 1. Transition Temperatures (T_{c1} and T_{c2}), Transition Enthalpies ($\Delta H_{en,1}$ and $\Delta H_{en,2}$), and Transition Entropies (ΔS_1 and ΔS_2) of C_{10}-DABCO-C_n-Br_2, and Ratios of the Conductivities Before (σ_l) and After (σ_h) the Transition at T_{c2}

Material	T_{c1} / °C	$\Delta H_{en,1}$ / kJ mol^{-1}	ΔS_1 / J/(mol deg)	T_{c2} / °C	$\Delta H_{en,2}$ / kJ mol^{-1}	ΔS_2 / J/(mol deg)	σ_h/σ_l
C_{10}-DABCO-C_{11}-Br_2	59	24.7	74	a)	a)	a)	a)
C_{10}-DABCO-C_{12}-Br_2	91	45.4	125	46	57.5	180	770
C_{10}-DABCO-C_{13}-Br_2	74	70.1	202	29	31.8	105	340
C_{10}-DABCO-C_{14}-Br_2	52	51.8	159	32	24.3	80	260
C_{10}-DABCO-C_{15}-Br_2	80	75.4	214	25	11.5	38	120
C_{10}-DABCO-C_{16}-Br_2	85	76.5	214	26, 32	25.3[b]	c)	190
C_{10}-DABCO-C_{17}-Br_2	85	80.0	222	24, 28	25.2[b]	c)	100
C_{10}-DABCO-C_{18}-Br_2	86	83.8	233	34	34.0	111	340
C_{10}-DABCO-C_{22}-Br_2	94	82.7	225	33	38.1	125	150

a) No phase transition occurred at T_{c2}. b) This value is a summation of the transition enthalpies at the two transition temperatures. The two signals could not be separated because of the proximity of the two transition temperatures. c) No correct ΔS_2 could be obtained.

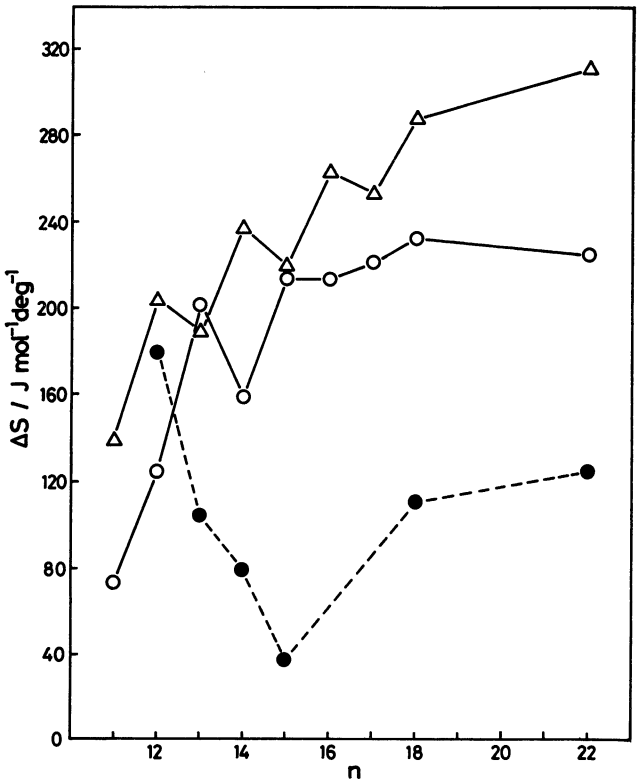

Fig. 6. The plots of the transition entropies against the carbon numbers of alkyl groups.
○: ΔS_1 of C_{10}-DABCO-C_n-Br_2, ●: ΔS_2 of C_{10}-DABCO-C_n-Br_2, △: ΔS of C_n-DABCO-C_n-Br_2.

numbers of the alkyl groups. This figure also shows the transition temperatures of the symmetric salts (C_n-DABCO-C_n-Br_2)[6] for the sake of comparison. Although complex behavior was observed for the T_{c1} of C_{10}-DABCO-C_n-Br_2 ($11 \leqq n \leqq 14$), the T_{c1}'s of C_{10}-DABCO-C_n-Br_2 ($15 \leqq n \leqq 22$) have a parallel relation to those of the symmetric salts; the former are slightly lower than the latter. The parallel relation suggests that the transition at T_{c1} is mainly governed by the longer alkyl chain of the two. On the other hand, T_{c2} decreases with the increase in the alkyl-chain length and levels off at around 30 °C for the DABCO salts, which possess longer alkyl chains than C_{12}. The differences between T_{c1}'s and T_{c2}'s were found to be in the range of 20—61 °C. Figures 5 and 6 plot the transition enthalpies ($\Delta H_{en,1}$ and $\Delta H_{en,2}$) and transition entropies (ΔS_1 and ΔS_2) respectively. These figures also show the transition enthalpies and transition entropies of the symmetric salts[6] for the sake of comparison. Since $\Delta H_{en,2}$ and ΔS_2 correspond to the transition enthalpy and the transition entropy from the metastable phase to the high temperature phase, the observed values are connected with dotted lines in these figures. $\Delta H_{en,2}$ and ΔS_2 are much smaller than $\Delta H_{en,1}$ and ΔS_1 respectively for C_{10}-DABCO-C_n-Br_2 ($n \geqq 13$). However, they are close to each other for C_{10}-DABCO-C_{12}-Br_2. The above results lead to the following assumptions for the phase transitions. The virgin sample (C_L)[10] possesses a close-packed crystal structure. This is confirmed by the IR absorption spectra, as will be described later. Therefore, T_{c1} is high, and $\Delta H_{en,1}$ and ΔS_1 are large, as a result of the considerable change in the crystal and molecular structures at the transition temperature. When it was once annealed[10] above T_{c1} and then cooled to room temperature, the conformational change in the alkyl chain and possibly the translational shift and rotational change of the molecule, all of which had been produced in the C_H phase, remained to some extent in the C_M phase at room temperature. This gave rise to a large number of disorders which facilitate the conformational, translational, and rotational movements of the molecule. Thus, when C_M was heated again, the phase transition due to these movements occurred at much lower temperatures (T_{c2}) than T_{c1}. From the Boltzmann relation, $\Delta S = R \ln W$, the ratios of the numbers of sites (W) before and after the phase transition can be estimated. W are estimated to be in the range of 10^6—10^{12} for the transitions at T_{c1} and in that of 10^2—10^9 for the transitions at T_{c2}. The fact that the former are much larger than the latter also exhibits how the metastable phase contains the above-mentioned disorder. In other words, the structural change from C_L to C_H is much larger than that from C_M to C_H. This results in the smaller enthalpy and entropy changes at T_{c2} than at T_{c1}.

Infrared Absorption Spectroscopy. The temperature dependence of the IR absorption spectra was measured for the KBr pellet sample in order to obtain more information on the phase transition and on the metastable phase. We have already reported the temperature dependences of the IR spectra of C_{14}-DABCO-C_{14}-Br_2[6] and C_{14}-DABCO-C_{16}-Br_2[7] as typical examples of the symmetric and unsymmetric DABCO salts respectively. In the former case, an abrupt change in the IR spectra was observed at the transition temperature. The spectral change was reversible, which was consistent with the DSC measurements. The band progressions in the low-temperature phase disappeared completely at the transition temperature. This was explained by the conformational change in the alkyl groups above the transition temperature. In the latter case, the band progressions disappeared at T_{c1} and were recovered again at lower temperatures (T_{c2}) than T_{c1}; $T_{c2} < T_{c1}$. These observations show the existence of the metastable phase in the latter case. Thus, the change in the IR spectra of the symmetric bis(quaternary salt) was quite different from that of the unsymmetric bis(quaternary salt). In order to see the effect of the difference in the carbon numbers of the two alkyl groups on the IR spectra, we measured the temperature dependence of the IR spectra of C_{10}-DABCO-C_{22}-Br_2, which possesses the largest difference in the

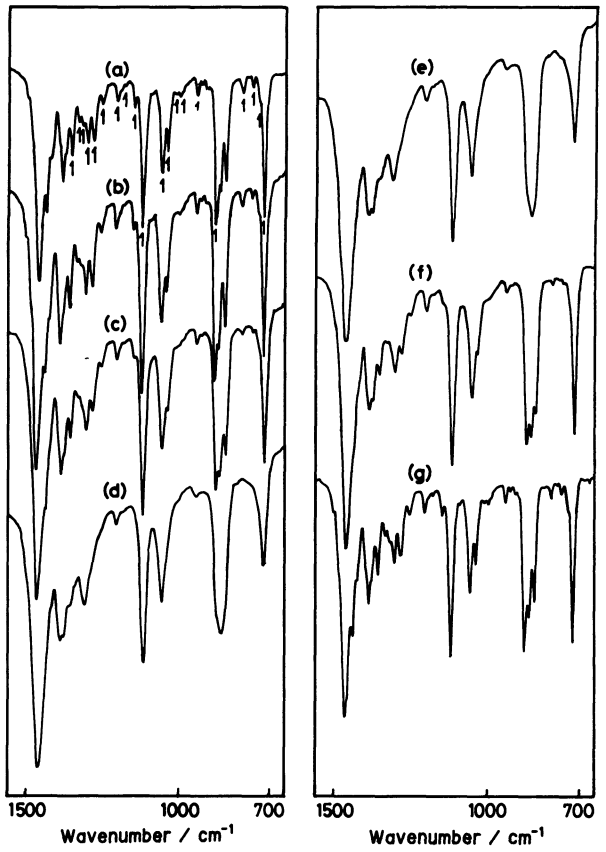

Fig. 7. Temperature dependence of the IR absorption spectra of C_{10}–DABCO–C_{22}–Br_2 for KBr disk sample obtained by heating the sample from room temperature to 94 °C, and then by cooling from 94 °C to 23 °C. The arrows in the spectrum (a) show the band progressions of the two alkyl groups.
(a): 29 °C, (b): 71 °C, (c): 90 °C, (d): 94 °C, (e): 70 °C, (f): 23 °C, (g): kept overnight at room temperature.

carbon numbers of the two alkyl groups.

Figure 7 shows the temperature dependence of the IR absorption spectra of C_{10}–DABCO–C_{22}–Br_2 for the KBr disk sample when the sample was heated from room temperature to 94 °C and then cooled to room temperature. The resulting IR spectra are shown sequentially from the upper left to the lower right. The IR spectra of the virgin sample[10] at 29 °C (a) exhibited the several structures shown by the arrows. The absorption positions of these structures were compared with the band progressions of n-$C_{11}H_{24}$ and n-$C_{23}H_{48}$,[11] which have the same numbers of CH_2 units as the alkyl groups of C_{10}–DABCO–C_{22}–Br_2. The good coincidence leads to the conclusion that the structures in Fig. 7 may be assigned to the band progressions of the two alkyl groups. The band progressions originating from 720 cm^{-1} are known as the CH_2-rocking mode. Since a single absorption was observed at 720 cm^{-1}, the molecules of the DABCO salts seem to possess a parallel-packed layered structure in the crystal.[12]

The absorption spectra at 29 °C (a) and 71 °C (b) were not very different. When the temperature of the sample approached T_{c1}, all of the absorptions were broadened (see Spectrum (c) at 90 °C), but the band progressions could still be seen. However, all of the band progressions disappeared at T_{c1} (94 °C) (d). This shows that the *trans*-zigzag conformation of the alkyl group of the low-temperature phase is destroyed at T_{c1}. When the temperature of the sample was lowered after it had once been raised above T_{c1}, no band progression appeared between T_{c1} and T_{c2}. For example, the IR Spectra (b) and (e) were measured at almost the same temperature, but they were quite different; Spectrum (b) exhibited the band progressions, but (e) did not show them. This is consistent with the free energy-temperature relation shown in Fig. 3, because Spectra (b) and (e) correspond to the C_L and C_H phases respectively. The *trans*-zigzag conformation of the alkyl chain is still destroyed in Spectrum (e). Only after the temperature had been lowered below T_{c2} (33 °C) did the band progressions appear again (see Spectrum (f)). Comparing Spectrum (a) with (f), however, the latter are broader than the former. This suggests that the conformational disorder still exists in (f). When the sample was left overnight at room temperature, the spectrum gradually became shaper to give Spectrum (g), which can not be differentiated from Spectrum (a). Thus, it is clear that the conformational change in the alkyl chain takes place slowly at room temperature. This is a distinct difference from C_n–DABCO–C_{n+2}–Br_2 ($10 \leqq n \leqq 16$), reported previously.[7] The band progressions recovered quickly below T_{c2} for these systems after they had once been heated above T_{c1}. Although Spectra (a) and (g) could not be differentiated from each other, their DSC results were quite different; the annealed sample[10] was converted to the metastable phase, but exceptionally, it did not go back to the stable phase.[9] A similar change in the IR absorption spectra was also observed for the other materials (C_{10}–DABCO–C_n–Br_2, $13 \leqq n \leqq 18$). However, the metastable phases of these materials are converted slowly to the stable phase by keeping the sample at room temperature. The conversion process could not be followed by IR spectroscopy, because the two phases possess identical IR absorption spectra. The powdered X-ray diffraction gave a distinct difference between the stable and metastable phases; the former gave sharp diffraction patterns, but the latter gave broader ones. Thus, the crystallinity of the latter is lower than that of the former.

Bromide-anion Conductivities. All of the samples have already been confirmed as bromide-anion conductors.[5,6,7] Ionic conductivities were measured for the compressed pellet samples by an AC method.[5,6] The temperature dependences of the bromide-anion conductivities were measured while raising the

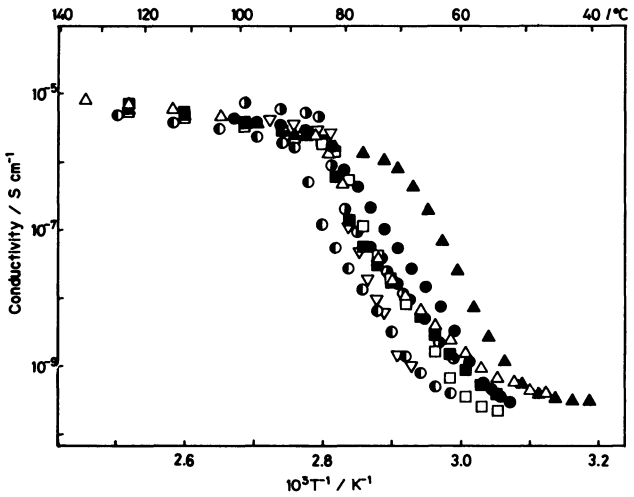

Fig. 8. Temperature dependences of the bromide-anion conductivities of the virgin samples (C_{10}–DABCO–C_n–Br_2).
●: n=12, △: n=13, ▲: n=14, □: n=15, ■: n=16, ◐: n=17, ◑: n=18, ▽: n=22.

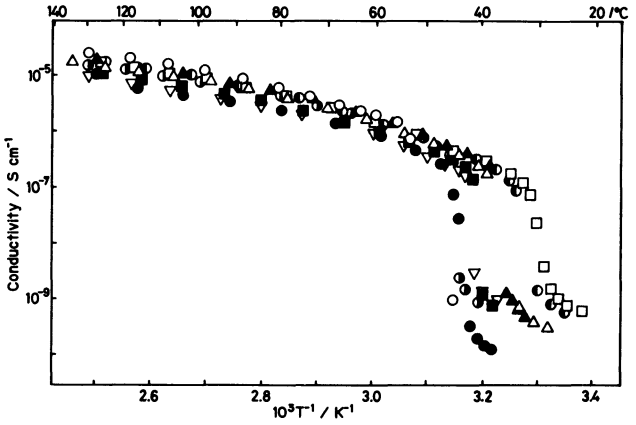

Fig. 9. Temperature dependences of the bromide-anion conductivities of the annealed samples (C_{10}–DABCO–C_n–Br_2).
○: n=11, ●: n=12, △: n=13, ▲: n=14, □: n=15, ■: n=16, ◐: n=17, ◑: n=18, ▽: n=22.

temperature of the sample slowly (0.5 °C min^{-1}) from room temperature. Conductivities less than 10^{-9} S cm^{-1} are below the limit of our measurements. Since the materials (C_{10}–DABCO–C_n–Br_2, $n \geqq 12$) exhibited phase transitions at T_{c1} and T_{c2}, we focused our attention mainly on the conductivity changes at these transition temperatures. The conductivity changes at around T_{c1} were measured for the virgin samples[10] dried in a vacuum overnight at room temperature. On the other hand, the conductivity changes at around T_{c2} were measured for the samples dried in a vacuum overnight above T_{c1}. Thus, the samples had already been converted to the metastable phase before the measurements. The proton conduction due to moisture seems to be negligible after the complete drying procedure.

Figure 8 shows the temperature dependences of the bromide-anion conductivities of the virgin samples.[10] Most of them consist of gradual increases in the conductivities in the low-temperature range and slow increases in the high-temperature range. Conductivity jumps like C_n–DABCO–C_n–Br_2,[6] C_n–DABCO–C_{n+2}–Br_2,[7] and the present materials in the metastable phase (see below) were not observed except for C_{10}–DABCO–C_{11}–Br_2. Thus, the conductivity change below the transition temperature is much broader than in the previous systems. The behavior in the low-temperature range was classified phenomenologically into two cases for C_{10}–DABCO–C_n–Br_2: (1) a considerable increase in the conductivity occurs below T_{c1} (n=12, 15, 16, 17, 18, 22), and (2) T_{c1} is located in the temperature range of the gradual increase in the conductivity (n=13, 14). At any rate, gradual increases in the conductivities occurred over wide temperature ranges. This suggests that the local movement of the alkyl chain sets in more than twenty degrees below T_{c1} for the virgin samples. Regarding the high-temperature phase, a considerable conformational movement of the alkyl group occurs. Thus, the activation energy of the conductivity was low (about 30 kJ mol^{-1}) as a result of the formation of a large number of transport channels of the bromide anion.

Figure 9 shows the temperature dependence of the bromide-anion conductivities of the annealed samples.[10] Unlike the case of the virgin samples,[10] an abrupt increase in the bromide-anion conductivities was observed at around T_{c2}. Part of Table 1 shows the ratios of the conductivities before (σ_l) and after (σ_h) the phase transitions; i.e., σ_h/σ_l. The σ_h/σ_l values were found to be in the range of 100—1380. Thus, they are smaller than those of C_n–DABCO–C_n–Br_2[6] and C_n–DABCO–C_{n+2}–Br_2.[7] If we define T_{c2}* as the middle point of the conductivity jump,[14] the following relations are obtained: T_{c2}*<T_{c2} for n=11, 12, and T_{c2}<T_{c2}* for $13 \leqq n \leqq 22$. The differences between T_{c2} and T_{c2}* were found to be in the range of 3—11 °C. The above relations suggest that the conductivity jumps begin before the considerable structural change for n=11, 12, and do after the change for $13 \leqq n \leqq 22$. It is noteworthy that the conductivities above T_{c1} of the virgin sample and those above T_{c2} of the annealed sample lie on the same σ–T curve. Figure 10 shows the temperature dependences of the bromide-anion conductivities of C_{10}–DABCO–C_{18}–Br_2 for the virgin sample and for the annealed sample as a typical example of this observation. Thus, the F–T relation in Fig. 3 is clearly demonstrated by Fig. 10. Since the ratios of the sites (W) before and after the phase transition are very large, as has been described before, the conformational change in the alkyl group seems to occur at every site of the CH_2 units. This gives rise to a large number of voids, which facilitate the bromide-anion transport above the transition temperature.

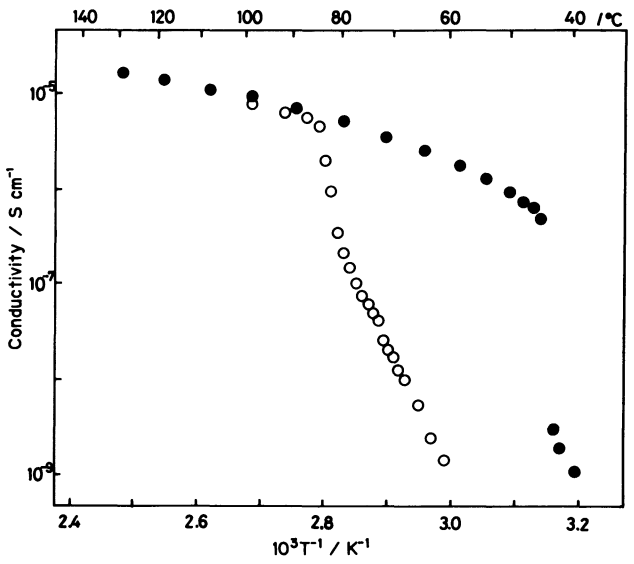

Fig. 10. Temperature dependences of the bromide-anion conductivities of C_{10}–DABCO–C_{18}–Br_2 for the virgin and annealed samples.
○: Virgin sample, ●: annealed sample.

Summary. Phase transitions of the unsymmetric bis(quaternary alkyl bromide) salts of DABCO (C_{10}–DABCO–C_n–Br_2, $11 \leqq n \leqq 22$) were studied by means of the measurements of the DSC, the IR absorption spectra, and the bromide-anion conductivities. The DSC measurements revealed the existence of a metastable phase. The metastable phase was found to be converted gradually to the stable phase for $13 \leqq n \leqq 18$ when the sample was kept at room temperature. The larger the difference in the carbon numbers of the two alkyl groups, the faster the conversion rate. The stable phase was not recovered from the metastable phase for $n=12$ and 22. The temperature dependence of the IR absorption spectra showed that the band progressions in the low-temperature phase disappeared above T_{c1} and appeared again at T_{c2}. The band progressions of the annealed sample became sharper when it was kept at room temperature. These facts can be explained by the conformational change in the alkyl group above the transition temperature, by the existence of the metastable phase, and by the slow recovery of the stable conformation at room temperature. Abrupt increases in the bromide-anion conductivities by two to three orders of magnitude were found at around T_{c2} for the annealed samples. The conductivity jump could be explained by the formation of voids attributable to conformational disorder above the transition temperature. On the other hand, the virgin sample did not show any conductivity jump. Instead, they exhibited broad conductivity changes below T_{c1}.

We are grateful to Professor Shigekazu Kusabayashi and Dr. Shunsuke Takenaka, Faculty of Engineering, Osaka University, for the use of the DSC apparatus.

References

1) D. S. Newman, D. Hazlett, and K. F. Mucker, *Solid State Ionics*, **3/4**, 389 (1981); M. Fujimoto, T. Nogami, and H. Mikawa, *Chem. Lett.*, **1982**, 547.

2) M. Fujimoto, T. Nogami, and H. Mikawa, *Solid State Ionics*, **11**, 313 (1984).

3) J. Shimizu, T. Nogami, and H. Mikawa, *Solid State Ionics*, **14**, 153 (1984).

4) K. Imamura, T. Nogami, and H. Mikawa, *Solid State Ionics*, **17**, 77 (1985).

5) J. Shimizu, T. Nogami, and H. Mikawa, *Solid State Commun.*, **54**, 1009 (1985).

6) J. Shimizu, K. Imamura, T. Nogami, and H. Mikawa, *Bull. Chem. Soc. Jpn.*, **59**, 1443 (1986).

7) K. Imamura, J. Shimizu, and T. Nogami, *Bull. Chem. Soc. Jpn.*, **59**, 2699 (1986).

8) There are a large number of metastable phases ($C_{M'}$, $C_{M''}$, $C_{M'''}$, ··· etc) between C_L and C_M. They differ mainly in the conformation of the alkyl groups and in their crystallinity.

9) One exception to this rule was C_{10}–DABCO–C_{22}–Br_2. The conversion rate from C_M to C_L was too slow to be followed for this material.

10) The virgin sample and the annealed sample are defined as the DABCO salts synthesized and the DABCO salts which have been heated above T_{c1} at least once respectively.

11) R. G. Snyder, *J. Mol. Spectrosc.*, **4**, 411 (1960); R. G. Snyder and J. H. Schachtschneider, *Spectrochim. Acta*, **19**, 85 (1963).

12) If the adjacent molecules are located in different orientations along the long axes of the molecules in the solid, crystal-field splitting must be observed at around 720 cm^{-1} (see Ref 13).

13) R. F. Holland and J. R. Nielsen, *J. Mol. Spectrosc.* **8**, 383 (1962).

14) The T_{c2}*'s of C_{10}–DABCO–C_n–Br_2 are as follows: 49 °C ($n=11$); 43 °C ($n=12$); 36 °C ($n=13$); 37 °C ($n=14$); 30 °C ($n=15$); 40 °C ($n=16$); 32 °C ($n=17$); 45 °C ($n=18$); 42 °C ($n=22$).